SAND2015-8624C

A Reduced Iwan Model That Includes Pinning for Bolted Joint Mechanics

M. R. W. Brake*
Sandia National Laboratories†
P.O. Box 5800, MS 1070
Albuquerque, NM 87185-1070, USA

September 29, 2015

Abstract

Bolted are joints are prevalent in most assembled structures; however, predictive models for the behavior of these joints do not yet exist. Many calibrated models have been proposed to represent the stiffness and energy dissipation characteristics of a bolted joint. In particular, the Iwan model put forth by Segalman and later extended by Mignolet has been shown to be able to predict the response of a jointed structure over a range of excitations once calibrated at a nominal load. The Iwan model, however, is not widely adopted due to the high computational expense of implementing it in a numerical simulation. To address this, an analytical, closed form representation of the Iwan model is derived under the hypothesis that upon a load reversal, the distribution of friction elements within the interface resembles a scaled version of the original distribution of friction elements. Additionally, the Iwan model is extended to include the pinning behavior inherent in a bolted joint.

Keywords: Joint Mechanics; Iwan Model; Pinning; Friction; Hysteresis

1 Introduction

One of the great remaining challenges in classical structural dynamics and solid mechanics is the prediction of the behavior of a jointed connection. Despite the prevalence of jointed connections in engineering structures, predictive models do not exist for several reasons: in most applications there is no penalty for over designing a joint to ensure that it survives most realistic loading scenarios, the physics to predict the behavior of a joint is reliant upon an improved understanding of friction (which is a nontrivial undertaking), and what joint models do exist are often computationally burdensome (which results in analysts favoring simplistic and hopefully conservative representations instead). However, in several industries (aerospace, defense, automotive, etc.) there is becoming a pressing need to better understand the behavior of a jointed connection. In many of the pertinent applications, the jointed connections are part of a system that will only be fabricated a small number

*mrbrake@sandia.gov

†Sandia National Laboratories is a multi-program laboratory managed and operated by Sandia Corporation, a wholly owned subsidiary of Lockheed Martin Corporations, for the U.S. Department of Energy's National Nuclear Security Administration under Contract DE-AC04-94AL85000.

of times and that has strict weight and space limits (increasing the penalty for over designing the joint). Conventional approaches to modeling the joint, due to harsh loading environments and nonlinearities, often are not as conservative as an analyst anticipates. In fact, the use of linear models, calibrated at low excitation levels, significantly over predict the energy dissipation and joint stiffness at high load levels. Consequently, a number of failures have been reported in recent years that are related to bolted joints (see, for instance, (Deckstein and Traufetter 2012)).

The present research is motivated by one particular class of joint models that are used in finite element analysis as well as analytical mechanics and reduced order models: the Iwan model. The broad category of constitutive models referred to as Iwan models are used to model dissipative behavior with a single degree of freedom. These models originally were applied to elastic-plastic material responses (Iwan 1966; Iwan 1967) and have more recently been adapted to joint mechanics (Segalman 2005; Segalman and Starr 2004). In particular, the four-parameter Iwan model (Segalman 2005) regularizes the joint interface to be represented by a single degree of freedom. The four-parameter Iwan model is, essentially, a constitutive model that describes the hysteretic behavior of micro- and macroslip across a jointed interface and replaces the kinematics of the adjacent interfacial surfaces with a nonlinear constitutive model. The model's constitutive parameters can be populated either with representative experimental data or deduced from fine mesh finite element analysis. The constitutive formulation is fundamentally that of a Preisach model and has basis in (Bauschinger 1886; Masing 1926; Prandtl 1928; Ishlinskii 1944; Iwan 1966; Iwan 1967). More recently, the Iwan model has been extended to be considered in modal space (as opposed to physical coordinates) (Deaner et al. 2013)

One difficulty present in the implementation of the Iwan model is its high computational cost. The Iwan models used for the analysis of bolted joints are based on a discretized set of dry friction sliders (Segalman 2005). This discretization leads to the need to store the individual state of each dry friction slider in the model, effectively increasing the degrees of freedom from one to an arbitrarily large number. In what follows, a reduced formulation of the Iwan model is derived based on the assumption that when a load reversal occurs, the state of each dry friction slider is reset (this assumption is discussed in Section 2.2.1. While this is a subtle change from the four-parameter Iwan model formulated in (Segalman 2005), both the new and old models are still approximations that can be calibrated to fit the data accurately, and the resulting model thus does not lose applicability from this new assumption.

2 Analytical Development

Conceptually, there are three distinct regimes for the model, as can be seen in Fig. 1: microslip ($0 \leq \delta < \phi_{MAX}$), macroslip ($\phi_{MAX} \leq \delta < \delta_P$), and pinning ($\delta_P \leq \delta$). In what follows, these three regimes will be calculated as part of two separate calculations: one calculation for the force due to the Iwan model, which includes micro- and macroslip, and one calculation for the pinning force.

2.1 Pinning Force

The pinning force occurs when the shank of the bolt engages the edge of the through hole (of diameter $2\delta_P$) in which it is located. This contact is thus between two cylindrical surfaces. If no plasticity is assumed to occur, this can be modeled using Hertz's (Johnson 1985) elastic contact

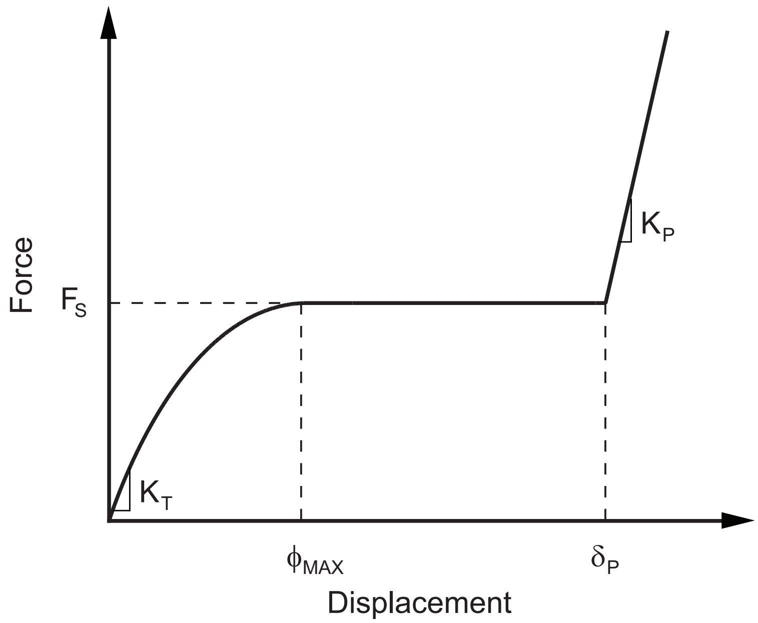

Figure 1: Illustrative drawing of the constitutive force F for a bolted joint as a function of displacement δ.

formulation for two cylinders

$$F_{PIN} = \frac{\pi}{4} E^* L d. \tag{1}$$

For this formulation, E^* is the effective modulus of the two materials in contact (each having elastic modulus E_j and Poisson's ratio ν_j)

$$E = \left(\frac{1-\nu_1^2}{E_1} + \frac{1-\nu_2^2}{E_2} \right)^{-1}. \tag{2}$$

The engagement length of the bolt's shank with the through hole (i.e. the height of the hole) is L, and d is the interference/contact displacement of the two surfaces. As (1) is linear in d, F_{PIN} can be expressed as a spring force $F_{PIN} = K_P d$ with stiffness

$$K_P = \frac{\pi}{4} E^* L. \tag{3}$$

All parameters needed to define K_P are based on material and geometric properties, which can be easily determined.

2.1.1 Relation of Relative and Global Displacements for the Iwan and Pinning Forces

In what follows, the relative displacement u is defined to be positive in the slip direction. Additionally, δ_0 is defined to be the global displacement of the system at the start of a slip event (e.g. a load reversal), and F_0 is defined to be the force due to the Iwan element at the start of a slip event. In order to relate the force due to the Iwan model and the force due to pinning,

$$\delta = \delta_0 + u. \tag{4}$$

This relationship establishes the constraint that at $u \geq \delta_P - \delta_0$, the pinning force is engaged

$$F_{PIN} = \pm H|u + \delta_0 \mp \delta_P| K_P(u + \delta_0 \mp \delta_P). \tag{5}$$

2.2 Four-Parameter Iwan Model Overview

For both the micro- and macroslip regimes, the Iwan model is proposed. As a starting point, the four parameter Iwan model developed in (Segalman 2005) is used. In that research, the constitutive representation for the Iwan forces is

$$F_{IWAN} = \int_0^\infty \rho(\phi)\,(u(t) - x(t,\phi))\,\mathrm{d}\phi, \tag{6}$$

which describes a distribution $\rho(\phi)$ of dry friction sliders (Jenkins elements) such as shown in Fig. 2. Note that in (Segalman 2005), the global displacement U is used in place of the relative displacement u; this substitution is made, though, without loss of generality in what follows due to the introduction of F_0 and δ_0, mentioned above. The j^{th} slider has instantaneous displacement $x_j = x(t, \phi_j)$, and transitions from sticking to sliding at a displacement of $x_j = \phi_j$. The choice of distribution $\rho(\phi)$ is a nontrivial task, and several choices are discussed in what follows. For the

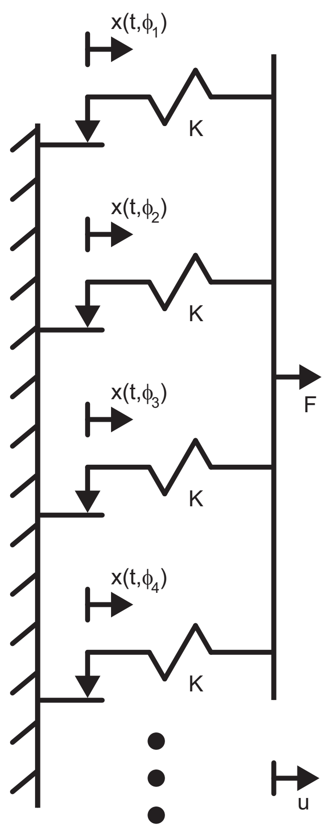

Figure 2: Illustrative drawing of an Iwan model as a parallel arrangement of dry friction sliders.

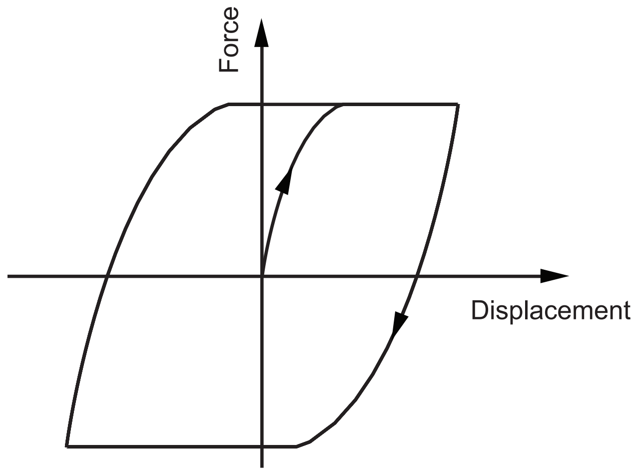

Figure 3: Illustrative drawing of a typical hysteresis curve for a four-parameter Iwan model described by (Segalman 2005).

model proposed in (Segalman 2005), the general form of the hysteresis loop is illustratively shown in Fig. 3.

The four-parameter Iwan model of (Segalman 2005) is subject to the two Masing conditions (which are both visible in Fig. 3): the forward and backward curves are reflections of one another and are scaled to fit between the initiation of the loading point and the force for macroslip, and that if a trajectory intersects the curve of a previous loading cycle, then it will change to follow the previous curve. In what follows, the first Masing condition is exploited: a displacement in the negative direction is the same as a displacement in the positive direction with a change of coordinates. The second Masing condition, though, due to possible transitions from microslip to macroslip to pinning, is neglected. By assuming that this condition can be neglected, the need for a burdensome approach that tracks the history of previous loading cycles, can be eliminated from this reduced formulation (a challenge that is evident in models such as (Smallwood, Gregory, and Coleman 2001; Segalman and Starr 2004)).

The distinguishing feature of the Iwan model is the proposed distribution of Jenkins elements $\rho(\phi)$, each element of which slips once they have been stretched a distance ϕ. In (Segalman 2005), the proposed distribution (shown in Fig. 4(a)) is

$$\rho(\phi) = R\phi^{\chi}\left(H(\phi) - H(\phi - \phi_{MAX})\right) + S\delta(\phi - \phi_{MAX}) \tag{7}$$

$$R = \frac{F_S(\chi + 1)}{\phi_{MAX}^{\chi+2}\left(\beta + \frac{\chi+1}{\chi+2}\right)} \tag{8}$$

$$S = \frac{F_S}{\phi_{MAX}}\frac{\beta}{\beta + \frac{\chi+1}{\chi+2}} \tag{9}$$

$$\phi_{MAX} = \frac{F_S(1 + \beta)}{K_T\left(\beta + \frac{\chi+1}{\chi+2}\right)}, \tag{10}$$

with Heaviside step function $H(\cdot)$ and Delta function $\delta(\cdot)$. In this formulation, $3+\chi$ is the energy dissipated per cycle of small amplitude oscillation. Thus, $-1 < \chi \leq 0$ in this model. The distribution ρ is a power law relationship that is truncated at ϕ_{MAX} with a Delta function. The ratio of the stiffness of the Delta function portion of the distribution S to the power law portion of the distribution R is defined as β

$$\beta = \frac{S}{R\phi_{MAX}^{\chi+1}/(\chi+1)}. \tag{11}$$

Note that with the definition of β, the model of (Segalman 2005) can be posed in terms of F_S, K_T, χ, and β, as opposed to a different set of parameters that are more difficult to directly measure (e.g. F_S, R, S, and ϕ_{MAX}). The relationships of Eqs. 8-10 are developed in (Segalman 2005) with this ease of model parameter determination in mind.

Observe that with the definition of u the quantity from Eq. 6

$$u - x(t,\phi) = \begin{cases} u & \text{if slider } \phi \text{ is stuck} \\ \phi & \text{if slider } \phi \text{ is sliding.} \end{cases} \tag{12}$$

Thus, define

$$\Gamma(u,\phi) = u - x(t,\phi) = \begin{cases} u & u < \phi \\ \phi & u \geq \phi. \end{cases} \tag{13}$$

Substituting Γ and ρ into Eq. 6 yields

$$F_{IWAN} = \int_0^{\phi_{MAX}} \Gamma(u,\phi) R\phi^{\chi} \mathrm{d}\phi + S\Gamma(u,\phi_{MAX}). \tag{14}$$

Based on Γ, this can be broken into two integrals

$$F_{IWAN} = \int_0^{u} R\phi^{\chi+1} \mathrm{d}\phi + \int_u^{\phi_{MAX}} uR\phi^{\chi} \mathrm{d}\phi + S\Gamma(u,\phi_{MAX}), \tag{15}$$

which has solution

$$F_{IWAN} = R\left(\left(\frac{1}{\chi+2} - \frac{1}{\chi+1}\right)u^{\chi+2} + \frac{\phi_{MAX}^{\chi+1}}{\chi+1}u\right) + S\Gamma(u,\phi_{MAX}). \tag{16}$$

Substituting Eqs. 8 and 9 gives the full expression for the Iwan forces

$$F_{IWAN} = \frac{F_S(\chi+1)}{\phi_{MAX}^{\chi+2}\left(\beta + \frac{\chi+1}{\chi+2}\right)}\left(\left(\frac{1}{\chi+2} - \frac{1}{\chi+1}\right)u^{\chi+2} + \frac{\phi_{MAX}^{\chi+1}}{\chi+1}u\right) + \frac{F_S}{\phi_{MAX}}\frac{\beta}{\beta + \frac{\chi+1}{\chi+2}}\Gamma(u,\phi_{MAX}). \tag{17}$$

In the limiting case of $u \geq \phi_{MAX}$, the Iwan force reduces to $F_{IWAN} = F_S$.

2.2.1 Considerations for Cyclic Loading

Two cases must be considered for the cyclic loading: loading to macroslip, and loading within the microslip regime. In loading to macroslip, all of the Jenkins sliders are, by definition, in slip. Thus the first Masing condition can be applied. For the first cycle of loading, it is assumed that $F_0 = 0$ and $\delta_0 = 0$. After the first cycle in which the joint is in macroslip, $F_0 = F_S$ (as F_0 doesn't include

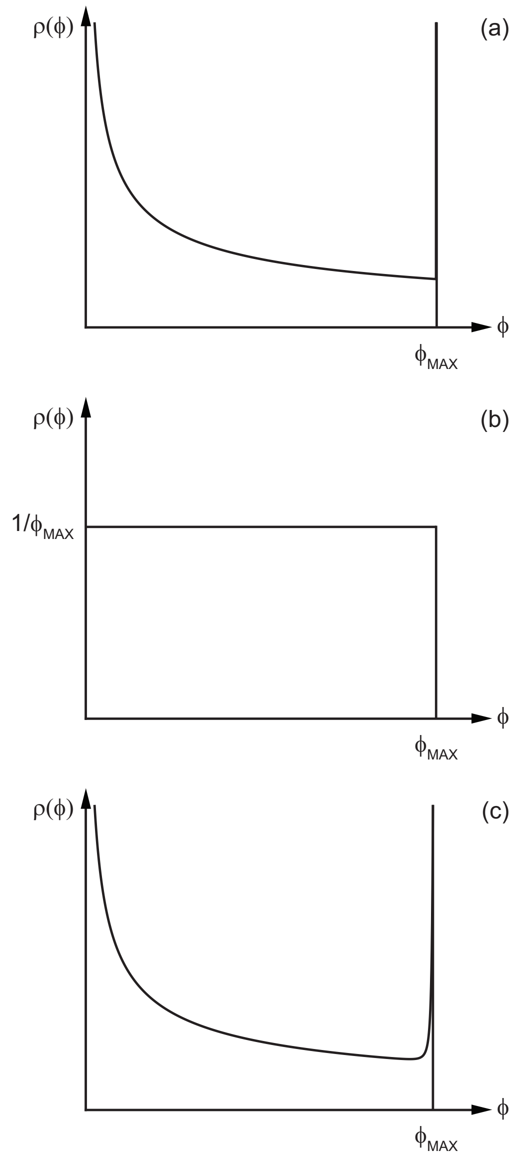

Figure 4: Illustrations of (a) the distribution of (Segalman 2005), (b) the uniform distribution of (Iwan 1966), and (c) Segalman's proposed distribution.

pinning forces), and each Jenkins element is fully stretched in the direction opposite from the new loading direction. For oscillations between two extremes (i.e. $-F_S$ and F_S), the first Masing condition (Segalman 2005; Jayakumar 1987) yields

$$F_+(u) = -F_S + 2F_{IWAN}\left(\frac{\delta - \delta_0}{2}\right) \tag{18}$$

$$F_-(u) = -F_S - 2F_{IWAN}\left(\frac{\delta_0 - \delta}{2}\right). \tag{19}$$

The forces F_+ and F_- are for positive and negative loading cycles respectively. Essentially, Eqs. 18 and 19 have the form

$$F_{\pm} = \mp F_S \pm \gamma F_{IWAN}\left(\frac{\pm\delta \mp \delta_0}{\gamma}\right), \tag{20}$$

where γ scales the function appropriately.

In many vibratory environments, however, the limits of oscillation are not necessarily between the two extreme values. Thus, an incomplete case (e.g. never loading to the point of macroslip) must be considered. In the previously defined relative coordinate system for u, after a load reversal, $-F_0 > -F_S$, the Jenkins elements of strength ϕ are fully stretched in the direction opposite from the new loading direction for $\phi < u_0$, and are stretched a distance u_0 in the direction opposite from the new loading direction for $\phi > u_0$. As a result, Eq. 15 becomes

$$F_{IWAN} = \int_0^u R\left(\frac{\phi}{2}\right)^{\chi+1} \mathrm{d}\phi + \int_u^{\phi_M AX} uR\phi^{\chi}\mathrm{d}\phi + S\Gamma(u, \phi_{MAX}) - F_0, \tag{21}$$

for $u \leq 2u_0$, and, with $\psi = \phi - 2u_0$, for $u > 2u_0$

$$F_{IWAN} = \frac{1}{2^{\chi+1}}\int_0^{2u_0} R\phi^{\chi+1}\mathrm{d}\phi + \int_{2u_0}^{u} R\psi^{\chi+1}\mathrm{d}\psi + \int_u^{\phi_M AX} uR\phi^{\chi}\mathrm{d}\phi + S\Gamma(u, \phi_{MAX}) - F_0. \tag{22}$$

The form of Eq. 22 is a (nonlinearly) scaled version of Eq. 15. Thus, the hypothesis is proposed:

Hypothesis For an arbitrary load reversal, there is a new distribution of Jenkins elements that are now stuck that approximately resembles a scaled version of the original distribution of Jenkins elements.

As a first order approximation of the new distribution, a linear scaling function is used in which γ is bounded by $0 < \gamma \leq 2$. This leads to the functional form

$$F_{SLIDING} = \begin{cases} F_0 + \frac{F_S - F_0}{F_S} F_{IWAN}\left(u\frac{F_S}{F_S - F_0}\right) & \text{loading} \\ F_0 - \frac{-F_S - F_0}{-F_S} F_{IWAN}\left(-u\frac{-F_S}{-F_S - F_0}\right) & \text{reverse loading} \end{cases} \tag{23}$$

This is rewritten as

$$F_{SLIDING} = F_0 + \frac{F_S \mp F_0}{F_S} F_{IWAN}\left(\pm u\frac{F_S}{F_S \mp F_0}\right). \tag{24}$$

This relationship is predicate on F_0 being a global value such that $-F_S \leq F_0 \leq F_S$. The complete formulation for the RIPP joint model can now be expressed as

$$F_{RIPP} = F_{PIN} + F_{SLIDING}. \tag{25}$$

In the case of $\delta_0 \geq \delta_P - \phi_{MAX}$, this implies that macroslip is not necessary to achieve pinning. It should be noted, however, that the force F_0 should be determined solely from $F_{SLIDING}$ in order for the model to be consistent.

2.2.2 Comparison With the Discrete Four-Parameter Iwan Model

As a verification of the analytical RIPP joint formulation, the RIPP joint model (25) is compared to the discretized four-parameter Iwan model of (Segalman 2005) on which it is based in Fig. 5. The parameters for (Segalman 2005) are chosen based on a 304 Stainless Steel lap joint, such as found in (Segalman et al. 2009), and are listed in Table 1. The range for the displacement to calculate the hysteresis curve is specified as ±2.25 mm. Outside of the pinning region, the two curves are coincident. Near the transition from microslip to macroslip, the discretization of (Segalman 2005) is evident under high magnification (as the curve appears faceted), but at the scale shown the two models are in complete agreement.

Property	Value
Tangential Stiffness, K_T	1.5×10^7 N/m
Macroslip Force, F_S	4 kN
Dissipation Exponent, χ	-0.5
Stiffness Ratio, β	0.005
Pinning Stiffness, K_P	10^7 N/m
Pinning Clearance, δ_P	2 mm

Table 1: Joint Parameters.

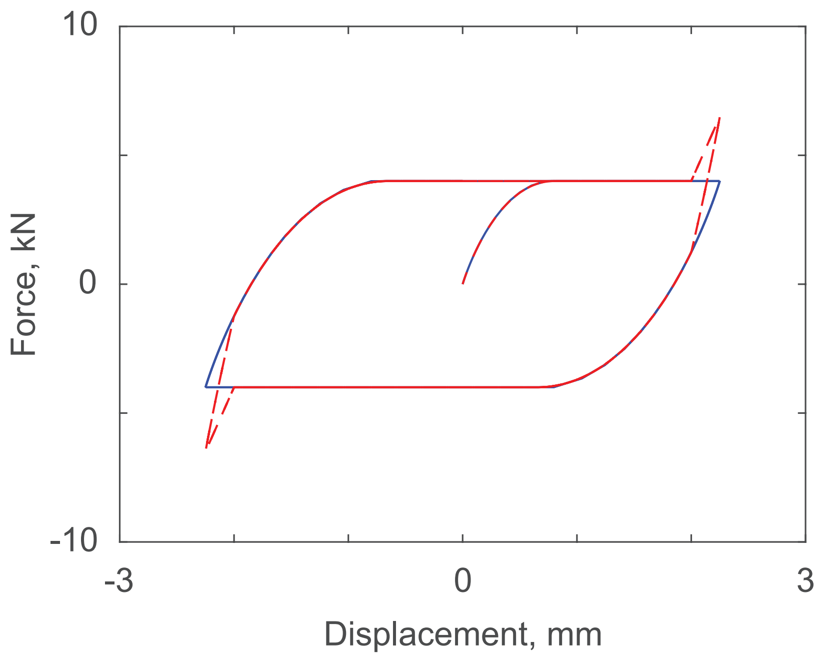

Figure 5: Hysteresis curves for the discretized four-paramter Iwan model of (Segalman 2005) (—), and the RIPP joint model (– –).

2.3 Extension to the Five-Parameter Iwan Model

The five-parameter Iwan model, championed by Mignolet (Wang and Mignolet 2014), belongs to a class of split Iwan models in which the response is split into two regimes. The fifth parameter is defined as the ratio between dynamic μ_D and static μ_S friction

$$\theta = \frac{\mu_D}{\mu_S}. \tag{26}$$

The conceptual split in this model is that once a Jenkins element begins to slide, it is governed by dynamic friction rather than the static friction that governed it in the stick state. The proposed distribution $\rho(\phi)$, though, remains the same. Consequently, the Iwan force becomes

$$F_{IWAN} = \theta \int_0^u R\phi^{\chi+1} \mathrm{d}\phi + \int_u^{\phi_{MAX}} uR\phi^{\chi} \mathrm{d}\phi + S\Gamma(u, \phi_{MAX}). \tag{27}$$

In the limiting case of $\theta = 1$, this reduces to Eq. 15. As before, the solution follows that

$$F_{IWAN} = R\left(\left(\frac{\theta}{\chi+2} - \frac{1}{\chi+1}\right)u^{\chi+2} + \frac{\phi_{MAX}^{\chi+1}}{\chi+1}u\right) + S\Gamma(u, \phi_{MAX}). \tag{28}$$

Substituting R and S yields the final form of the Iwan force equation for the five-parameter Iwan model

$$F_{IWAN} = \frac{F_S(\chi+1)}{\phi_{MAX}^{\chi+2}\left(\beta + \frac{\chi+1}{\chi+2}\right)}\left(\left(\frac{\theta}{\chi+2} - \frac{1}{\chi+1}\right)u^{\chi+2} + \frac{\phi_{MAX}^{\chi+1}}{\chi+1}u\right) + \frac{F_S}{\phi_{MAX}} \frac{\beta}{\beta + \frac{\chi+1}{\chi+2}}\Gamma(u, \phi_{MAX}). \tag{29}$$

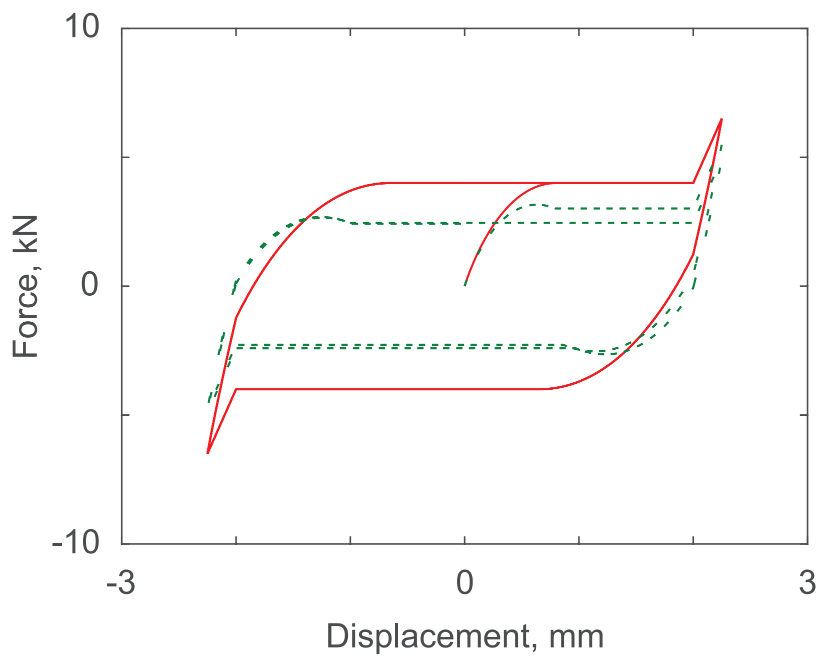

Figure 6: Hysteresis curves for the RIPP joint model of the four-parameter Iwan model (—), and of the five-parameter Iwan model with $\theta = 0.75$ (– –).

In the limiting case of $u \geq \phi_{MAX}$,

$$F_{IWAN} = F_S \frac{\beta + \theta \frac{\chi+1}{\chi+2}}{\beta + \frac{\chi+1}{\chi+2}}, \tag{30}$$

which is less than F_S for $\theta < 1$.

In Fig. 6, the RIPP joint model of the four-parameter Iwan model is compared to the RIPP joint model of the five-parameter Iwan model with $\theta = 0.75$ and all other parameters the same as before. Both models exhibit the same tangent stiffness immediately after a load reversal; however the five-parameter model has a lower peak force due to $\theta < 1$. One unexpected consequence of this (coupled with the neglecting of the second Masing condition, as mentioned above) is that the maximum and minimum forces vary from one loading cycle to the next.

2.4 Extension to the Uniform Iwan Distribution

In (Iwan 1966), the Iwan element is formulated with a uniform distribution for ρ (Fig. 4(b)). The width of the distribution for the present work is taken to be ϕ_{MAX}, with a height of $1/\phi MAX$. This distribution leads to the Iwan force

$$F_{IWAN} = \int_0^{\phi_{MAX}} \frac{c}{\phi_{MAX}} \Gamma(u, \phi) \mathrm{d}\phi. \tag{31}$$

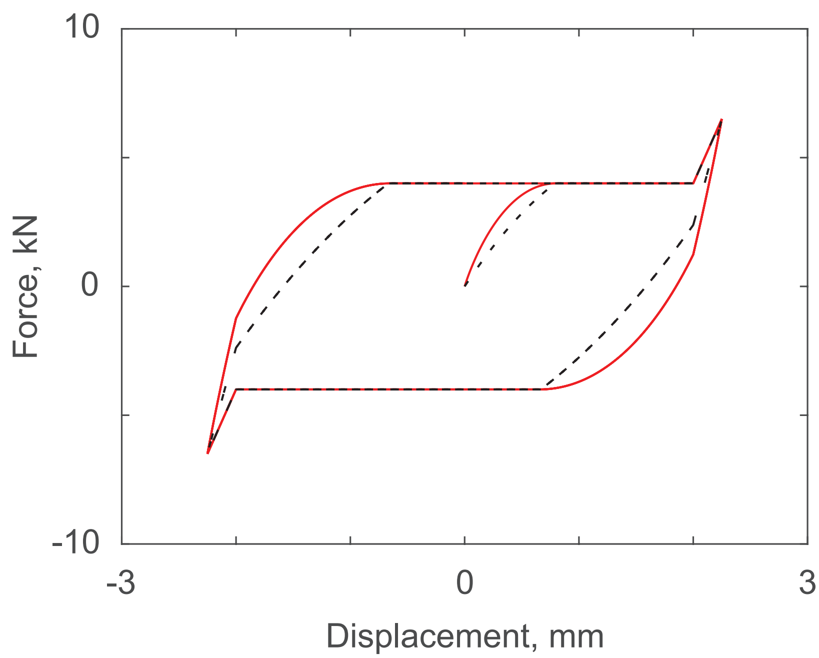

Figure 7: Hysteresis curves for the RIPP joint model of the four-parameter Iwan model (—), and of the uniform distribution Iwan model (– –).

The constant c is determined by setting the resulting solution equal to F_S, yielding

$$F_{IWAN} = \begin{cases} \frac{2F_S}{\phi_{MAX}}\left(u - \frac{u^2}{2\phi_{MAX}}\right) & u < \phi_{MAX} \\ F_S & u \geq \phi_{MAX}. \end{cases} \quad (32)$$

Using the same parameters as from Fig. 5, Fig. 7 compares the hysteresis curves for the RIPP joint model of the four-parameter Iwan model to that of the uniform distribution Iwan model. Due to the uniform distribution for $\rho(\phi)$, the tangent stiffness appears much lower than for the four-parameter Iwan model. By definition, the macroslip forces and pinning behavior is the same for the two models though.

3 Summary

The analytical representation of the discretized Iwan model is formulated in this research for several different friction models: the four-parameter distribution of Segalman, the five-parameter distribution of Mignolet, and the uniform distribution originally used by Iwan. The advantage of an analytical representation of the Iwan model is a dramatic improvement in computational time compared to the discretized Iwan model developed in (Segalman 2005). The key hypothesis that enables the analytical formulation is that on a load reversal, there is a new distribution of sliders in sticking and slipping states that resembles a scaled version of the original distribution of sliders.

References

Bauschinger, J. (1886). "On the Change of Position of the Elastic Limit of Iron and Steel Under Cyclic Variations of Stress". In: *Mitt. Mech. Tech. Lab. Munchen* 13, pp. 1–115.

Deaner, B. J. et al. (2013). "Investigation of Modal Iwan Models for Structures with Bolted Joints". In: *31st International Modal Analysis Conference (IMAC XXXI)*. Garden Grove, CA.

Deckstein, D. and G. Traufetter (2012). "Weight Loss for Superjumbos: The A380 and the Aviation Engineering Dilemma". In: *Der Spiegel*.

Ishlinskii, A. Y. (1944). "Some Applications of Statistical Methods to Describing Deformations of Bodies". In: *Izvestiya Akademii Nauk SSSR* 9, pp. 580–590.

Iwan, W. D. (1966). "A Distributed-Element Model for Hysteresis and its Steady State Dynamic Response". In: *ASME Journal of Applied Mechanics* 33, pp. 893–900.

— (1967). "On a Class of Models for the Yielding Behavior of Continuous and Composite Systems". In: *ASME Journal of Applied Mechanics* 34, pp. 612–617.

Jayakumar, P. (1987). *Modeling and Identification in Structural Dynamics*. Doctoral Dissertation. California Institute of Technology.

Johnson, K. L. (1985). *Contact Mechanics*. Cambridge: Cambridge University Press.

Masing, G. (1926). "Self-Stretching and Hardening for Brass". In: *Proceedings of the Second International Congress for Applied Mechanics*, pp. 332–335.

Prandtl, L. (1928). "Ein Gedankenmodell zur kinetischen Theorie der festen Korper". In: *Zeitschrift fur Angewandte Mathematik und Mechanik* 8, pp. 85–106.

Segalman, D. J. (2005). "A Four-Parameter Iwan Model for Lap-Type Joints". In: *ASME Journal of Applied Mechanics* 72, pp. 752–760.

Segalman, D. J. and M. J. Starr (2004). *Relationships Among Certain Joint Constitutive Models*. Technical Report SAND2004-4321. Sandia National Laboratories, Albuquerque, NM.

Segalman, D. J. et al. (2009). *Handbook on Dynamics of Jointed Structures.* Technical Report SAND2009-4164. Sandia National Laboratories, Albuquerque, NM.

Smallwood, D. O., D. L. Gregory, and R. G. Coleman (2001). "A Three Parameter Constitutive Model for a Joint which Exhibits a Power Law Relationship Between Energy Loss and Relative Displacement". In: *72nd Shock and Vibration Symposium.* Destin, FL.

Wang, X. Q. and M. P. Mignolet (2014). "Stochastic Iwan-Type Model of a Bolted Joint: Formulation and Identification". In: *32nd International Modal Analysis Conference (IMAC XXXII).* Orlando, FL.